

Lymphocyte-Specific Protein Tyrosine Kinase (LCK) is Involved in the Aryl Hydrocarbon Receptor-Mediated Impairment of Immunoglobulin Secretion in Human Primary B Cells

Jiajun Zhou,^{*,†} Qiang Zhang,[‡] Joseph E. Henriquez,^{†,§} Robert B. Crawford,[†] and Norbert E. Kaminski^{*,†,§,1}

^{*}Department of Microbiology & Molecular Genetics; and [†]Institute for Integrative Toxicology, Michigan State University, East Lansing, Michigan 48824; [‡]Department of Environmental Health, Rollins School of Public Health, Emory University, Georgia 30322; and [§]Department of Pharmacology & Toxicology, Michigan State University, East Lansing, Michigan 48824

¹To whom correspondence should be addressed at Michigan State University, 1129 Farm Lane, Room 165G Food Safety and Toxicology building, East Lansing, MI 48824. Fax: 517-355-4603; E-mail: kamins11@msu.edu.

ABSTRACT

The aryl hydrocarbon receptor (AHR) is a cytosolic ligand-activated transcription factor involved in xenobiotic sensing, cell cycle regulation, and cell development. In humans, the activation of AHR by 2,3,7,8-Tetrachlorodibenzo-*p*-dioxin (TCDD), a high affinity AHR-ligand, impairs the secretion of immunoglobulin M (IgM) to suppress humoral immunity. However, the mechanisms bridging the activation of AHR and the impairment of IgM secretion by human primary B cells remain poorly understood. Recent transcriptomic analysis revealed upregulation of lymphocyte-specific protein tyrosine kinase (LCK) in AHR-activated human primary B cells. LCK is a well-characterized tyrosine kinase that phosphorylates critical signaling proteins involved in activation and cytokine production in T cells. Conversely, the role of LCK in human primary B cells is not well understood. In the current studies, we have verified the transcriptomic finding by detecting AHR-mediated upregulation of LCK protein in human primary B cells. We also confirmed the role of AHR in the upregulation of LCK by using a specific AHR antagonist, which abolished the AHR-mediated increase of LCK. Furthermore, we have confirmed the role of LCK in the AHR-mediated suppression of IgM by using LCK specific inhibitors, which restored the IgM secretion by human B cells in the presence of TCDD. Collectively, the current studies demonstrate a novel role of LCK in IgM response and provide new insights into the mechanism for AHR-mediated impairment of immunoglobulin secretion by human primary B cells.

Key words: AHR; LCK; human B cell; IgM; immunoglobulin; dioxin.

The aryl hydrocarbon receptor (AHR) is a cytoplasmic receptor that can be activated by environmental contaminants (Sorg, 2014; Sulentic and Kaminski, 2011). In addition to being an environmental sensor, the AHR also plays a role in regulating proliferation, cell growth, and cellular differentiation (Barouki *et al.*, 2007; Nguyen and Bradfield, 2008; Nguyen *et al.*, 2013). In the immune system (Abbott *et al.*, 1999; Bunger *et al.*, 2003; Schmidt

et al., 1996), the AHR plays a role in the expansion, maturation (Thurmond *et al.*, 2000) and differentiation of hematopoietic stem cells (Smith *et al.*, 2013). Specifically, the AHR is important for the differentiation and proliferation of T helper cells (Th₁₇), induction of IL-22 and the generation of T regulatory cells (T_{reg}) from CD4⁺ T cells (Veldhoen *et al.*, 2008, 2009). However, B lymphocytes are also a sensitive target for AHR activation as

evidenced by impairment of B-cell lineage commitment and suppression of humoral immune responses (Holsapple et al., 1986; Li et al., 2017a,b).

The AHR signaling pathway is capable of influencing immune responses. The AHR is a ligand-activated transcription factor belonging to the Per-AHR nuclear translocator (ARNT)-Sim superfamily of proteins. In the absence of ligand binding, the AHR remains quiescent bound to heat shock proteins (Hsp90), Ah receptor-associated protein-9 (Ara9), and cochaperone protein (p23) in the cytosol (Whitlock, 1990). Chaperone proteins, Hsp90 and Ara9, are critical chaperone proteins which maintain the AHR conformation for proper ligand recognition (Heid et al., 2000). Upon ligand binding, the AHR undergoes a conformational change, exposing the nuclear localization sequence at the N-terminal, dissociates from the chaperone proteins and translocates into the nucleus (Perdew, 1988). In the nucleus, the ligand-AHR complex heterodimerizes with the ARNT (Mimura et al., 1999) and is capable of binding dioxin responsive elements (DREs) within the regulatory regions of genes to positively or negatively influence gene transcription.

2,3,7,8-Tetrachlorodibenzo-*p*-dioxin (TCDD), a high affinity AHR ligand, has been used to study the physiological role of AHR in immune cells. AHR ligands (halogenated dibenzo-*p*-dioxins, dibenzofurans, and biphenyls) are highly lipophilic, stable and resistant to metabolism and their toxicity is dependent on binding to AHR (Bisson et al., 2009). The activation of AHR by TCDD can produce a wide range of toxic responses including hepatotoxicity and immune suppression in different animal species (Harper et al., 1991; Holsapple et al., 1986; Kerkvliet, 2002; Poland and Knutson, 1982; Sulentic and Kaminski, 2011). Previous studies from AHR null mice (Gonzalez and Fernandez-Salguero, 1998) and rats (Phadnis-Moghe et al., 2016) have shown resistance to hepatotoxicity, the induction of AHR gene battery, and suppression of humoral immune responses upon TCDD exposure (Fernandez-Salguero et al., 1997; Vorderstrasse et al., 2001). In the well-characterized mouse model, C57BL/6, the activation of AHR contributes to a decrease in synthesis of immunoglobulin M (IgM) (Schneider et al., 2008). Additionally, the activation of AHR contributes to the decrease of Pax5 and Blimp-1, important regulators of B-cell differentiation into antibody producing plasma cells (North et al., 2010). Studies using a human *in vitro* system revealed that AHR-mediated impairment of IgM secretion correlates with a decrease in Protein Kinase B (AKT) PKB and extracellular signal-regulating kinase (ERK), indicating ligand activation of AHR disrupts signal cascades that leads to decreased IgM secretion by human B cells (Lu et al., 2011).

The role of lymphocyte-specific protein tyrosine kinase (LCK) has not been well studied in B cells. However, LCK is a critical signaling molecule in T-cell receptor (TCR) and IL-2 receptor signaling. Upon ligand binding to the TCR, phosphorylation at the immunoreceptor tyrosine-based activation motif of the TCR then transfers the phosphate group to LCK on the Src homology 2 (SH2) domain (Roskoski, 2005). The phosphorylation of the SH2 domain facilitates recruitment and activation of ζ chain-associated protein kinase of 70 kDa (ZAP70), which in turn phosphorylates signal adaptors important for Ca^{2+} mobilization (Shi et al., 2013) and the activation of MAP kinase and NF-AT pathways for T-cell proliferation (Efremov et al., 2007). Upon TCR ligation, the activated LCK can phosphorylate the membrane-associated adaptor proteins LAT and VAV-1 (Bunnell et al., 2002). The activation of vesicular associated proteins LAT and VAV-1 play a critical role in vesicle transport and cytoskeleton remodeling. Whereas little is known concerning the role of LCK

in B cells, studies have indicated expression of LCK in B-1 cells (Griffin et al., 2011; Majolini et al., 1998) and an important role of LCK in B-cell receptor (BCR) signaling in chronic lymphocytic leukemia (CLL) cells, such that the increase of LCK has been implicated as a biomarker in CLL patients (Majolini et al., 1998; Talab et al., 2013). Interestingly, a recent transcriptomic analysis in our laboratory identified upregulation of LCK mRNA in AHR activated human primary B cells (Kovalova et al., 2017).

Previous studies have shown that AHR activation impairs immunoglobulin secretion by human primary B cells (Zhou et al., 2018). In the current studies, we have identified novel involvement of AHR-mediated upregulation of LCK in the impairment of immunoglobulin secretion by human primary B cells. These findings provide important insights into the molecular mechanism by which AHR activation impairs immunoglobulin secretion by human primary B cells.

MATERIALS AND METHODS

Chemicals and reagents. A 99.1% pure TCDD in dimethylsulfoxide (DMSO) was purchased from Accustandard, Inc. (New Haven, Connecticut). The DMSO was purchased from Sigma-Aldrich (St Louis, Missouri) and was used to dilute the TCDD. LCK small peptide inhibitor (EGQYpEEIP) and control peptide (EGQYEEIP) were purchased from GenScript (Piscataway, New Jersey). LCK inhibitor (RK24466) (CAS213743-31-8) was purchased from Sigma-Aldrich.

Cell culturing. CD40 ligand-L cells were obtained as a generous gift from Dr. David Sherr (Boston University). CD40 ligand-L cells are a mouse fibroblast cell line stably transfected with human CD40 ligand (CD40L). The cells were cultured in Dulbecco's Modified Eagle's Medium (ThermoFisher, Waltham, Massachusetts) supplemented with 10% bovine calf serum (ThermoFisher), 50 μM of 2-mercaptoethanol (ThermoFisher), and HT supplement (ThermoFisher). CD40 ligand-L cells were thawed 4 days before irradiation with 3500 rad of X-rays using X-Rad 320 (Precision X-Ray, Inc., North Branford, Connecticut) a day before coculturing with human primary B cells. CD40 ligand-L cells were seeded at a concentration of 1×10^4 cells/ml in 500 μl of media per well in 48-well tissue culture plates (Costar, Corning, New York) for the culture period. The expression of human CD40L on the surface of the cells was monitored routinely to select for high CD40L-expressing cells. Human peripheral blood B cells were cultured in Roswell Park Memorial Institute (RPMI) 1640 medium supplemented with 5% human AB serum (Valley Biomedical, Winchester, Virginia), and 50 μM of 2-mercaptoethanol. In all cases, cells were cultured in 5% CO_2 incubator at 37°C.

Human leukocyte packs and human B cells purification. Peripheral blood mononuclear cells (PBMCs) collected from anonymous platelet donors were obtained from Gulf Coast Regional Laboratories (Houston, Texas). All human leukocyte packs were tested to be negative for human immunodeficiency virus, hepatitis B virus, hepatitis C virus, and human T-lymphocyte virus before shipment. For each experiment, blood packs were diluted with HBSS and overlaid on Ficoll-Paque Plus density gradient (GE Healthcare, Piscataway, New Jersey) and centrifuged at $1300 \times g$ for 25 min with low acceleration and brake. The PMBCs were isolated postcentrifugation, washed, counted and subjected to magnetic column-based isolation that enriched $\text{CD}19^+ \text{CD}27^-$ naïve human B cells (more than 95% purity). This negative selection was conducted using the MojoSort human

naïve B cell isolation kit (Biolegend, San Diego, California) following the manufacturer's instructions. Purified human B cells at the concentration of 1×10^6 cells/ml were then treated with either 0.02% DMSO (VH) or various concentration of TCDD. The treated B cells were then activated by cocultured with sublethally irradiated CD40 ligand-L cells (1×10^4 cell/ml) in a 48-well cell culturing plate. Cells were cultured with recombinant human cytokines IL-2 (1 ng/ml), IL-6 (1 ng/ml) (Roche Applied Science, Indianapolis, Indiana), and IL-10 (4 ng/ml) (Biovision, Inc., Milpitas, California) for a total of 7 days. Soluble CD40L (100 ng/ml) (Enzo, Farmingdale, New York), IL21 (100 ng/ml), and IL2 (1 ng/ml) were added and cultured for 7 days with human B cells. B cells were activated with Pokeweed Mitogen (PWM) (15ug/ml) for 5 days. For LCK mRNA analysis, human B cells were treated with VH (0.02% DMSO) or TCDD (0.3, 3, and 30 nM) and cultured for a total of 3 days postactivation to verify the transcriptomic study (Kovalova et al., 2017). For all other studies, human purified naïve B cells were cultured for a total of 7 days. The LCK inhibitors were added on day 5 due to the upregulation of LCK protein expression. In the current study, responders were classified by a greater than 20% suppression of the IgM response in the presence of 10 nM TCDD when compared with VH control as measured by ELISA and ELISPOT.

Enzyme-linked immunospot assay. The number of IgM-secreting cells was quantified by ELISPOT. Briefly, multiscreen 96-well filter plates (Millipore, Burlington, Massachusetts) were coated with anti-human IgM antibody (5 µg/ml) (Sigma-Aldrich) overnight and subsequently blocked with 5% bovine serum albumin (BSA) (Sigma-Aldrich) for 2 h. The B cells were washed with RPMI 1640 two times, resuspended in RPMI 1640 containing 10% bovine calf serum (ThermoScientific, Waltham, Massachusetts) and incubated on the primary antibody-coated plates overnight at 37°C with 5% CO₂. Biotin-conjugated anti-human IgM antibody (Sigma-Aldrich) and, subsequently, streptavidin-horseradish peroxidase (HRP) (Sigma-Aldrich) was added for a 1-h incubation at 37°C with 5% CO₂. All incubations were followed with three washes with phosphate-buffered saline (pH 7.4) containing 0.1% Tween-20 (Sigma-Aldrich) and three washes with nanopure water. The spots were developed with an aminoethyl-carbazole staining kit (Sigma-Aldrich). The number of spots per well between 0.0001 and 9.6372 mm² were quantified via the Immunospot Software (Cellular Technology, Shaker Heights, Ohio) and normalized to the number of viable cells plated in each well.

Enzyme-linked immunosorbent assay. The amount of IgM secreted into the culture supernatant was quantified by sandwich ELISA. Briefly, Immulon 4 HBX 96-well microtiter plates (VWR International, Radnor, Pennsylvania) were coated with anti-human IgM antibodies (1 µg/ml; Sigma-Aldrich) overnight. Culture media collected from human B cells were incubated over primary antibody-coated plates for 90 min at 37°C with 5% CO₂ and was followed by overlaying to an anti-human IgM-HRP conjugate antibody (Sigma-Aldrich). Incubations were followed by washes with phosphate-buffered saline (pH 7.4) containing 0.05% Tween-20 (Sigma-Aldrich) and nanopure water. 2,2'-Azino-bis (3-ethylbenzothiazoline-6-sulphonic acid) (ABTS, Sigma-Aldrich) was then added as a colorimetric substrate for HRP. The rate of colorimetric change was quantified with a Synergy HT microplate reader (BioTek, Winooski, Vermont) at 405 nm for 1 h. Concentrations of IgM in media were calculated based on a standard curve created in each plate.

Gene expression analysis. The probe used in the studies was LCK (Hs00178427_m1). RNA was isolated using Qiagen RNeasy kits (Hilden, Germany) per the manufacturer's instructions. The RNA concentrations were determined by Nanodrop ND-1000 Scientific spectrophotometer (ThermoFisher) and 500 ng of RNA was used for the reverse-transcription using High Capacity cDNA RT-PCR kit by Applied Biosystems (Foster City, California). The cDNA was amplified using Applied Biosystems Taqman Gene Expression Assays. All quantitative real-time PCR reactions were performed on an Applied Biosystems model ABI Prism 7900 Sequence Detection System. Human 18S ribosomal RNA (Applied Biosystems) was used as an internal control. Fold change in gene expression was calculated using the $\Delta\Delta C_t$ method.

Flow cytometry. Antibodies used for flow cytometry were as follows: Alexa Fluor 647 anti-human LCK (Clone LCK-01, Biolegend), PE mouse anti-human LCK-pY505 (Clone 4/LCK-Y505, BD Biosciences, Franklin Lakes, New Jersey), Alexa Fluor 647 mouse anti-human pY319 ZAP70 (Clone 17A/POZAP70, BD Biosciences), Alexa Fluor 647 mouse anti-human pY292 ZAP70 (Clone J34-602, BD Biosciences). For flow cytometry staining, approximately 0.5×10^6 cells were harvested at the indicated time points and viable cells were identified by Fixable Live/Dead Near-IR dye (Life Technologies, Carlsbad, California) following the manufacturer's instructions prior to cell surface or intracellular staining. Surface Fc receptors were blocked using human AB serum before staining for surface and intracellular proteins. For surface staining, cells were resuspended in FACS buffer (1× phosphate-buffered saline, 1% BSA [San Diego, California] and 0.1% sodium azide, pH: 7.6) in the presence of 20% human AB serum. Antibodies were then added at the company specified concentrations and incubated at 4°C for 15 min and then fixed by incubation in the BD Cytotfix fixation buffer (BD Biosciences) for 10 min. For intracellular protein staining, cells that were previously fixed after surface staining were permeabilized with 1× BD PermWash buffer (BD Biosciences) for 30 min and incubated with antibodies for 30 min. For phospho staining, cells were incubated with phospho antibodies as instructed by BD Biosciences. In brief, cells were fixed using BD Cytotfix buffer for 10 min at 37°C then permeabilized using 1× of Perm buffer IV and stained for 1 h under continuous motion. Cells were then washed three times with 0.5X perm buffer and analyzed by flow cytometry. In all cases, cells were analyzed on BD FACSCanto II using FACS Diva software (BD Biosciences) and subsequently analyzed using FlowJo (Version 10, Treestar Software, Ashland, Oregon). Unless stated, cells were gated on singlets, live (as determined by Live/Dead dye) followed by gating on lymphocyte populations. Gates were drawn based on the unstimulated cells (resting human B cells, without CD40L and cytokine activation) or unstained cells as appropriate.

Mathematical modeling of the XNOR gate. The following algebraic equations were used to formulate an XNOR gate as shown in Figure 5A.

$$LCK = 100 \cdot \left(1 + \frac{TCDD}{K_1 + TCDD} \right) \quad (1)$$

$$LCK_a = LCK \cdot \frac{K_2}{K_2 + LCK_i} \quad (2)$$

$$IgM = \frac{100}{IgM_{max}} \cdot \frac{LCK_a^{n_3}}{K_3^{n_3} + LCK_a^{n_3}} \cdot \frac{K_4^{n_4}}{K_4^{n_4} + LCK_a^{n_4}} \quad (3)$$

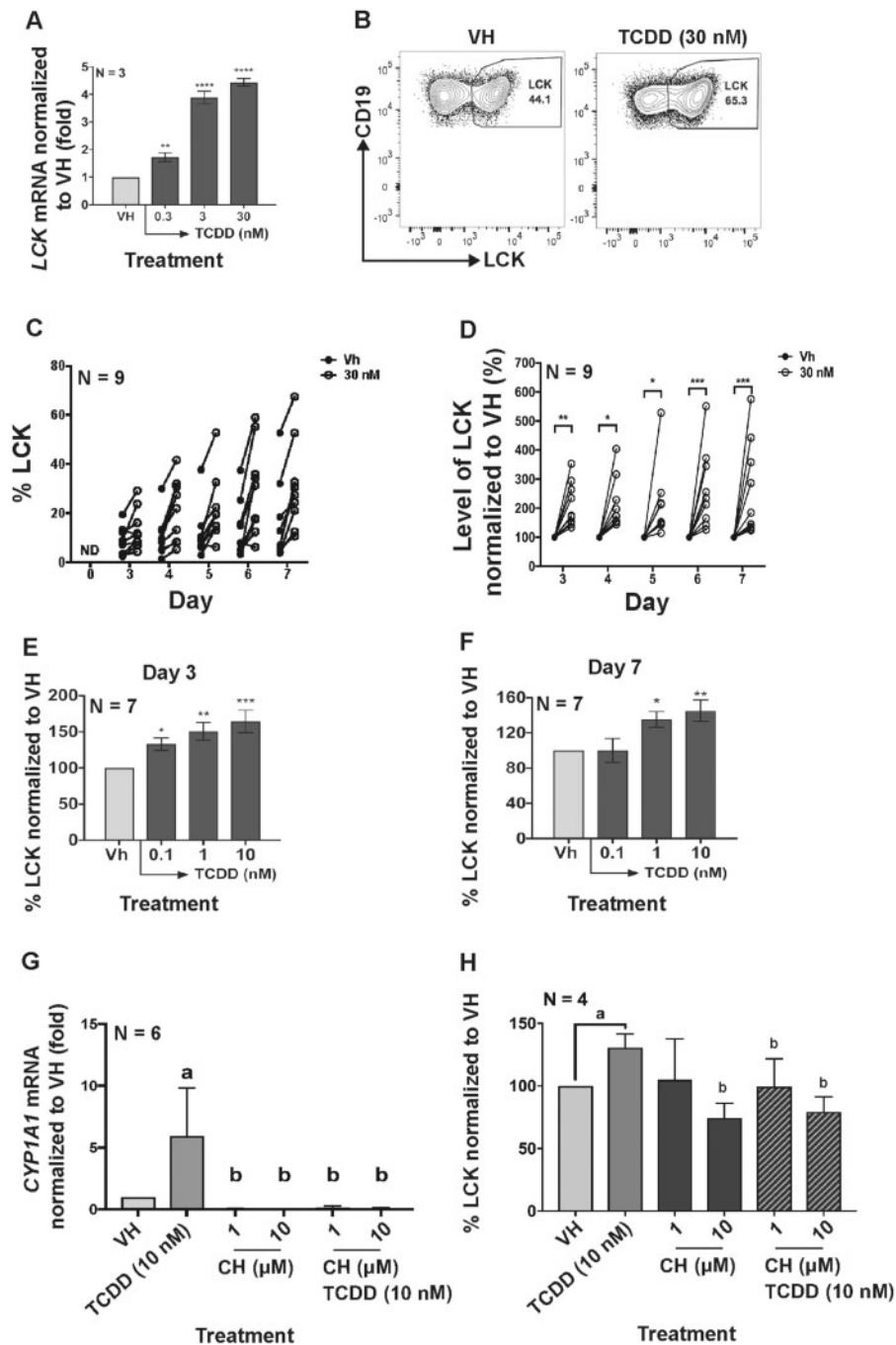


Figure 1. Aryl hydrocarbon receptor activation increased LCK expression in naïve human primary B cells. (A) Human B cells were treated with VH (0.02% DMSO), or TCDD (0.3, 3, and 30 nM) on day 0 and cultured for 3 days. mRNA levels of LCK as determined by real-time qPCR in B cells on day 3. (B) B cells were treated with VH (0.02% DMSO), or TCDD (30 nM) and cultured for 7 days. Flow cytometry dot plot of intracellular LCK in B cells with VH or TCDD treatment on day 7. Human B cells were treated with VH (0.02% DMSO) or TCDD (10 nM) for 7 days. Cells were collected on days 3–7 to analyze the LCK protein level. (C) Un-normalized percent positive LCK in B cells on day 0 (background) and days 3–7 post B-cell activation. (D) Normalized percent LCK positive B cells with VH or TCDD (30 nM) treatment from day 3 to day 7. Days 1 and 2 were excluded from the graph due to undetectable levels of LCK in human B cells. The circular dot indicates one individual human donor. Percent LCK positive B cells on (E) day 3 and on (F) day 7 measured by flow cytometry. Significant differences from VH control are indicated by * $p < .05$, ** $p < .01$, *** $p < .001$ by 1-way ANOVA following by Fisher’s LSD post hoc test. Naïve human primary B cells were treated with AHR antagonist, CH-223191 (CH) or a combination of both CH and TCDD (10 nM) on day 0. (G) CYP1A1 mRNA induction with TCDD, TCDD and CH-223191 (CH) treatments on day 1. (H) Percent LCK positive B cells on day 7. Two-way ANOVA followed by Fisher’s LSD post hoc test has been performed to compare all treatment groups. Significant differences from VH control are indicated by a ($p < .05$); significant differences from the TCDD group are indicated by b ($p < .05$). Results are presented as the normalized percentage compared to the VH group. “N” indicates the number of donors used in the study.

Note: LCK denotes the amount of LCK, which is induced by TCDD through a Michaelis-Menten kinetic process; LCK_i denote LCK inhibitor; LCK_a denotes LCK activity, which is proportional

to amount of LCK and is inhibited by LCK_i through an inhibitory form of Michaelis-Menten kinetic process. IgM denotes IgM secretion, which is normalized to the maximal amount of IgM

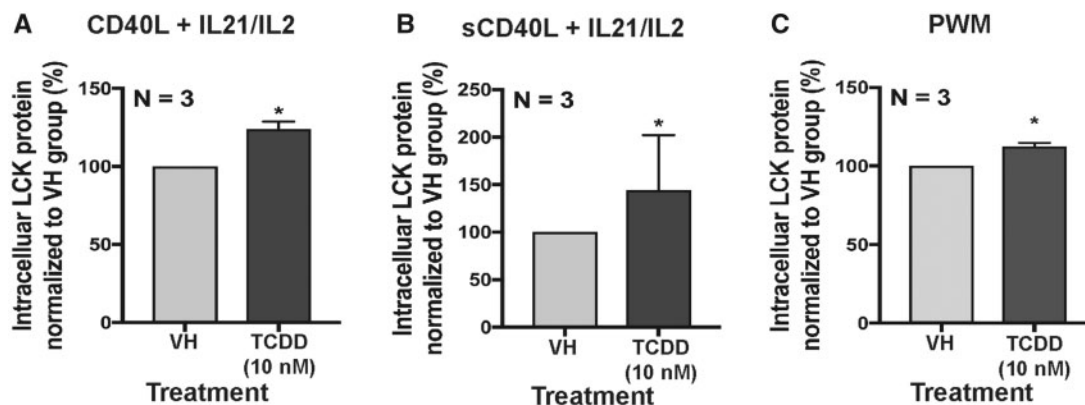


Figure 2. Aryl hydrocarbon receptor activation increased LCK in naïve human primary B cells activated with different stimuli. B cells were treated with VH (0.02% DMSO) or TCDD (10 nM) and activated by (A) CD40 ligand expressing L cells plus cytokines (IL-2 and IL-21); (B) soluble CD40 ligand plus cytokines (IL-2 and IL-21) or (C) pokeweed mitogen. The percent intracellular LCK positive B cells were quantified by flow cytometry on day 7. Significant differences from VH control are indicated by $p < .05$ by Student's *t*-test. Results are presented as the normalized percentage compared with the VH group. "N" indicates the number of donors used in the study.

secretion (ie, IgM_{max} , which is achieved when $LCK_a = 100$). The XNOR gate effect is modeled by the dual effects of LCK_a on IgM through the product of a stimulatory Hill function (parameterized by K_3 and n_3) and an inhibitory Hill function (parameterized by K_4 and n_4). The model was constructed and simulated with MATLAB (MathWorks, Natick, Massachusetts). To recapitulate the experimental TCDD and LCK inhibitor matrix data (Figs. 4G and 5B), the "fmincon" function in MATLAB was used for optimization with a cost function that measures the sum of the squared percentage difference between the data and mode output. The optimized parameters are as follows: $K_1 = 0.0886$, $K_2 = 1.30$, $K_3 = 80.96$, $K_4 = 120.88$, $n_3 = 13.81$, and $n_4 = 5.0$.

Statistical analysis. Student's *t*-test was used to compare VH control to TCDD treatment group. For multiple comparisons, 1-way ANOVA followed by Fisher's LSD post hoc test or 2-way ANOVA followed by Fisher's LSD post hoc test was used. Significant differences from VH control were indicated by $*p < .05$, $**p < .01$, $***p < .001$; $^a(p < .05)$ indicated significant differences to VH control; $^b(p < .05)$ indicates significant differences to the TCDD treatment group. The error bars represent standard deviation.

RESULTS

AHR Activation Increased LCK Expression in Human Primary B Cells
 Previous transcriptomic analysis identified the upregulation of LCK after AHR ligation in human primary B cells (Kovalova et al., 2017). In the current study, mRNA and protein levels of LCK were quantified *in vitro* in activated human primary B cells. LCK mRNA significantly increased with AHR activation on day 3 (Figure 1A). Likewise, the protein level of LCK increased significantly with AHR activation from day 3 to 7 (Figs. 1B–D). Additionally, the increase in the LCK protein levels corresponded with an increase in the TCDD concentration on day 3 and 7 (Figs. 1E and 1F). To determine if the increase in LCK was dependent on AHR activation, the AHR antagonist (CH-223191) was employed. The specificity of the antagonist (CH-223191) was verified by measuring the CYP1A1 mRNA induction with TCDD treatment (Figure 1G). Treatment with AHR antagonist abolished the TCDD-induced increase in LCK (Figure 1H). To ascertain whether upregulation of LCK by TCDD was specific to the mode of B-cell activation, B cells were activated in several different ways (CD40L fibroblast plus IL-2 and IL-21; by soluble CD40L plus IL-2 and IL-21 and by pokeweed mitogen).

Irrespective of the manner in which the cells were activated AHR activation resulted in upregulation of LCK in human primary B cells (Figs. 2A–C).

Upregulation of LCK Expression and Suppression of IgM Secretion Are Dependent on AHR Activation Within the First 24 h Post B-Cell Activation

Murine B cells are sensitive to suppression of IgM responses only when exposed to TCDD within the first 24 h post B-cell activation after which time they become refractory to TCDD-mediated suppression (Holsapple et al., 1986). Likewise, SKW-AhR⁺ 6.4 cells, a mature human B-cell line stably transduced to express AhR, exhibited the same temporal sensitivity to TCDD (ie, within first 24 h post B-cell activation) (Kovalova et al., 2016). In the present study, human naïve B cells were activated with CD40L expressing fibroblasts plus cytokines (IL-2, IL-6, and IL-10) and treated with TCDD (1 and 10 nM) on the day of activation (D0), day 1 (D1), day 2 (D2), or day 3 (D3) postactivation. On day 7, cells were collected and assayed for intracellular LCK protein levels, the number of IgM secreting cells, and the IgM concentration in culture supernatants (Figure 3). A temporal relationship was observed with respect to the TCDD-mediated increase in LCK protein levels, with the maximum percentage of LCK⁺ B cells being observed when TCDD was added to B cells on day 0 (Figure 3A). Similarly, the number of IgM secreting cells and the concentration of supernatant IgM was not affected by the TCDD treatment when TCDD was added to cultures on day-2 after B-cell activation or later (Figs. 3B and 3C), which is consistent with a number of prior reports (Kovalova et al., 2016; Tucker et al., 1986).

Specific LCK Inhibitors Restored IgM Secretion in the Presence of TCDD

The upregulation of LCK has been observed in CLL patients, and LCK has been suggested as a biomarker for CLL patients (Talab et al., 2013); however, little is known about the role of LCK in B-cell function. To more directly explore whether LCK plays a role in AHR-mediated suppression of IgM secretion, 2 different LCK-specific inhibitors were used as molecular probes. Based on our prior observation that TCDD treatment impaired IgM secretion on day 7 coupled with the kinetics of LCK induction (peak levels occurring around day 5), day 5 was selected for treatment with the LCK inhibitors. One LCK inhibitor is a well-characterized small peptide (PI) (EGQYpEEIP) that directly binds to the SH-2

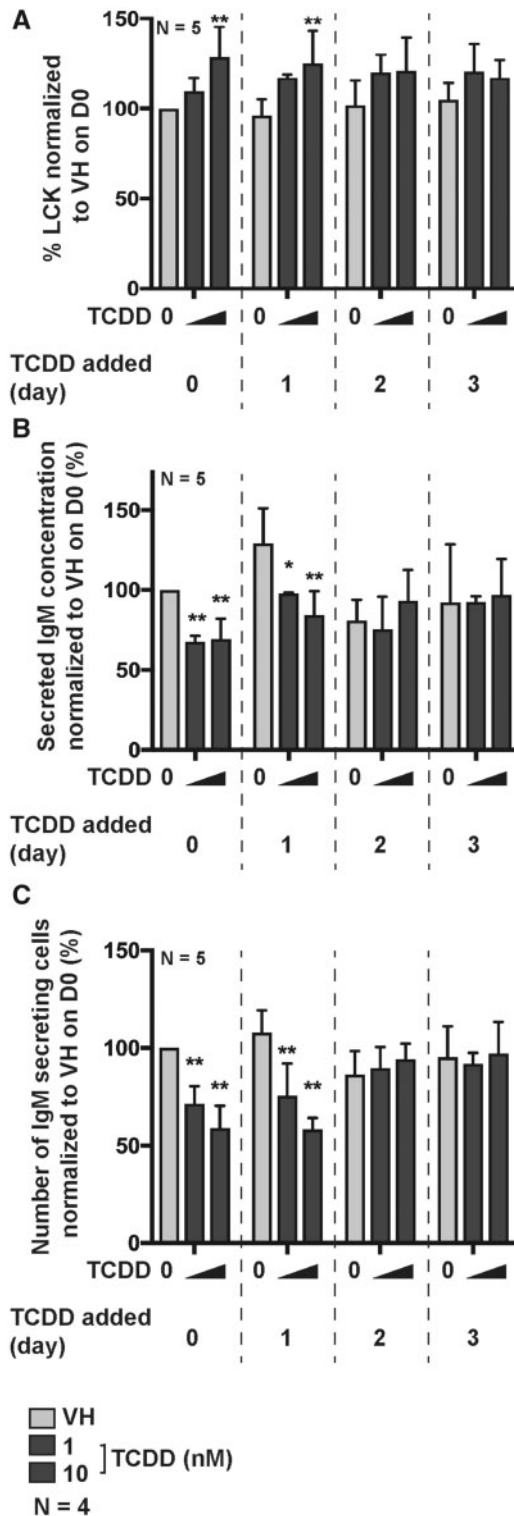


Figure 3. The upregulation of LCK expression and suppression of IgM secretion are dependent on AHR activation within the first 24 h post B-cell activation. B cells were activated by coculture with CD40 ligand expressing L cells plus cytokines (IL-2, IL-6, and IL-10) on day 0. Following activation, B cells were treated with VH (0.02% DMSO), or TCDD (1 and 10 nM) on day 0, 1, 2, or 3 and cultured for a total of 7 days. (A) Percent LCK positive B cells measured by flow cytometry on day 7. (B) IgM concentration in supernatants as quantified by ELISA; (C) the number of IgM secreting cells as quantified by ELISPOT on day 7. Significant differences from VH control are indicated by * $p < .05$, ** $p < .01$ by 1-way ANOVA following by Fisher's LSD post hoc test. Results are shown as the normalized percentage compared with the VH group. "N" indicates the number of donors used in the study.

domain of LCK. A control peptide (EGQYEEIP) was created to ensure the peptide was not affecting cell function. The percentage of LCK⁺ cells increased with the peptide control. No protection from the suppressive effects of TCDD on the number of IgM secreting cells or the amount of IgM secreted was observed with the control peptide. In contrast, in the presence of the PI, the percentage of LCK⁺ cells was increased by AHR activation but to a lesser extent than in the absence of the inhibitor (Figure 4A). The number of IgM secreting cells and the IgM concentration in supernatant was restored with the addition of PI (Figs. 4B and 4C). To further verify our finding, we employed a second and more potent small molecule LCK inhibitor (RK24466) with high LCK-binding affinity. The small molecule inhibitor (RK24466) possesses an IC50 of 1–2 nM for LCK in human cells, with minimal effects on other kinases. The results with RK24466 were similar to the PI LCK inhibitor such that the TCDD-mediated suppression of IgM secretion was restored to the VH control level with CAS treatment (Figs. 4D–F). Collectively, these findings show that LCK activity influences IgM secretion in response to AHR activation in B cells.

To better understand the interplay between AHR activation and LCK, we designed a matrix study with varying combinations of RK24466 and TCDD concentrations. In the absence of RK24466 there was a concentration-dependent suppression in IgM secretion (Figs. 4G and 4H). Similarly, in the absence of AHR activation, there was also a concentration-dependent suppression of IgM secretion with increasing concentrations of LCK inhibitor. Interestingly, for cells treated with both TCDD and LCK inhibitor simultaneously, their individual suppressive effects on IgM secretion, rather than being additive, were opposing, ie, the LCK inhibitor can restore IgM secretion in the presence of TCDD. When assessed using the number of IgM secreting cells, a similar profile of activity was observed.

The counterintuitive effects of TCDD and LCK inhibitor on IgM secretion are reminiscent of an XNOR logic gate, where the output is 1 (unsuppressed IgM secretion in this case) when both inputs are absent or present, whereas the output is 0 (suppressed IgM secretion) when only 1 of the 2 inputs is present (Figure 5A). The heat map in Figure 5B, which summarized the findings in Figure 4G, is clearly consistent with an XNOR gate I/O relationship. To interpret this interesting result, we formulated a simple XNOR gate model (see the section "Materials and Methods" for model details) by hypothesizing that the activity of LCK has a dual effect on IgM secretion and needs to reach an optimal level during the B-cell activation and differentiation process; deviation from this optimal level, either too high or too low, will lead to impaired IgM secretion (Figure 5D). Specifically, based on the effects of TCDD on LCK expression described above, we postulate that TCDD exposure alone results in an increase in total LCK activity from its optimal level. Conversely, LCK inhibitor alone results in a decrease in total LCK activity from its optimal level; however, when both are present in the appropriate ratio, their effects are opposing leading to near-optimal LCK activity (Figure 5E). As a result, IgM secretion exhibits an XNOR gate response profile (Figure 5F). After parameter optimization, our model quantitatively recapitulated the concentration response matrix effects observed experimentally (compare Figs. 5B and 5C).

AHR Activation Increased the Level of Active LCK

LCK activation is critical for TCR signaling and cytokine secretion (Hui and Vale, 2014). Upon TCR activation, the phosphorylation of the inhibitory site (Tyr505) on LCK is dephosphorylated, which in turn allows the activation of LCK

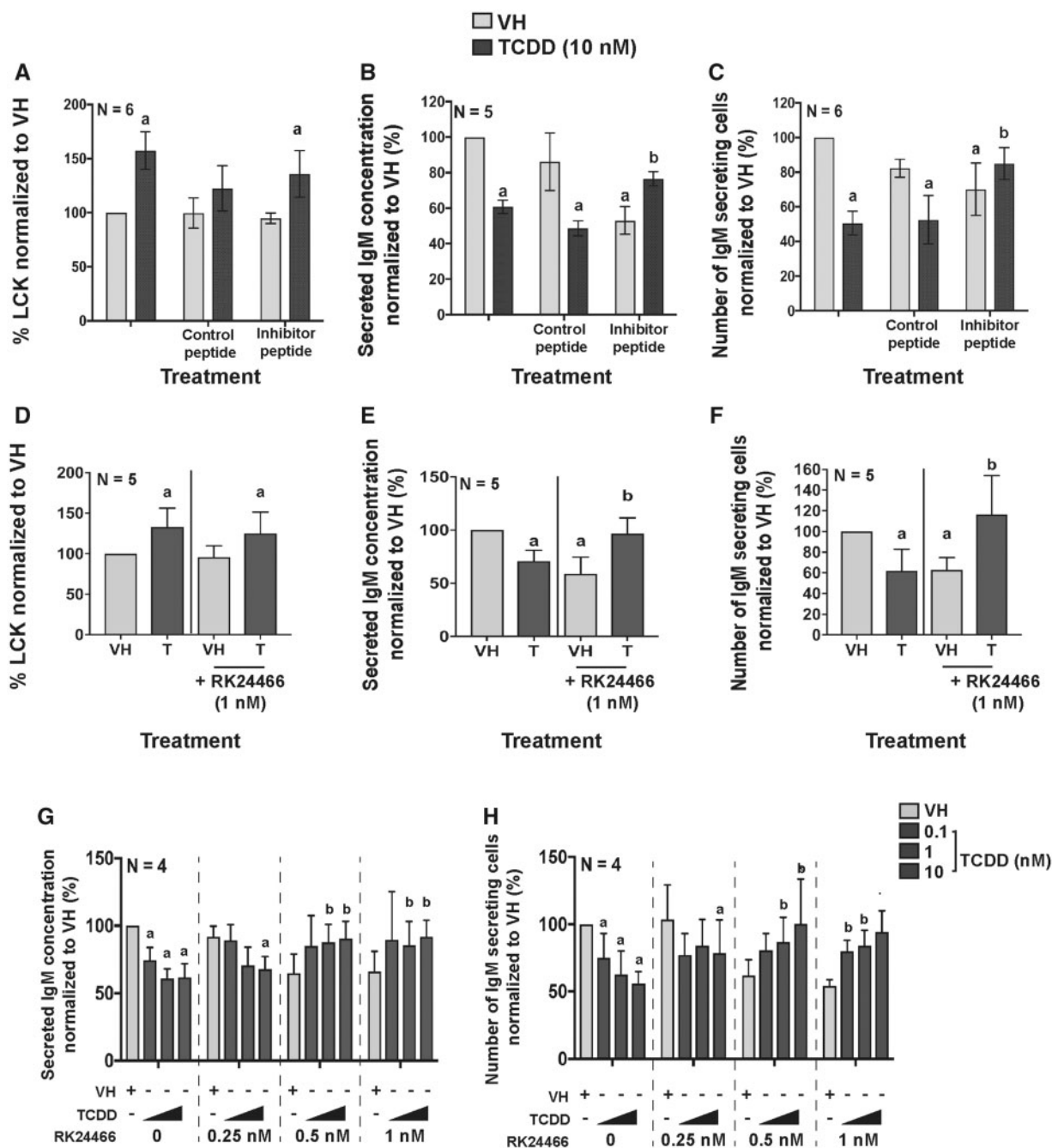


Figure 4. LCK inhibitors restored IgM secretion in the presence of TCDD. B cells were treated with VH (0.02% DMSO), or TCDD (10 nM) and activated by coculture with CD40 ligand expressing L cells plus cytokines (IL-2, IL-6, and IL-10) for 7 days. On day 5, the LCK inhibitor (EGQYpEEIP) or control peptide (EGQYEEIP) was added to the cell cultures. (A) Percent LCK positive human B cells measured by flow cytometry on day 7. (B) IgM concentration in supernatants as quantified by ELISA; and (C) the number of IgM secreting B cells as quantified by ELISPOT on day 7. On day 5, the LCK inhibitor (RK24466) was added to the cell cultures and the cells were harvested on day 7. (D) Percent LCK positive B cells measured by flow cytometry on day 7. (E) IgM concentration as quantified by ELISA on day 7. (F) The number of IgM secreting cells as quantified by ELISPOT on day 7. B cells were treated on day 0 with TCDD (0.1, 1, and 10 nM) and LCK inhibitor (0, 0.25, 0.5, and 1 nM) and cultured for 7 days. Cells were collected to quantify (G) IgM concentration in supernatant; and (H) the number of IgM secreting cells on day 7. Significant differences from the TCDD (10 nM) group without LCK inhibitor are indicated by a ($p < .05$) by 2-way ANOVA followed by Fisher's LSD post hoc test; significant differences from the VH group without LCK inhibitor are indicated by b ($p < .05$) by 2-way ANOVA followed by Fisher's LSD post hoc test. Results are presented as the normalized percentage compared with the VH group. "N" indicates the number of donors used in the study.

(Hui and Vale, 2014). Once activated, LCK phosphorylates ZAP70 at Tyr319 and Tyr292 (Di Bartolo et al., 1999; Wang et al., 2010), which then phosphorylates downstream signal adaptors. In the current studies, the activity of LCK was examined using phospho-intracellular staining targeting the inhibitory

phosphorylated site (Try505) on LCK (Hui and Vale, 2014) measured by flow cytometry. Before examining the activity of LCK, we quantified the percent of ZAP70⁺ B cells following treatment with VH or TCDD. The activation of AHR slightly increased intracellular ZAP70 only with highest TCDD concentration

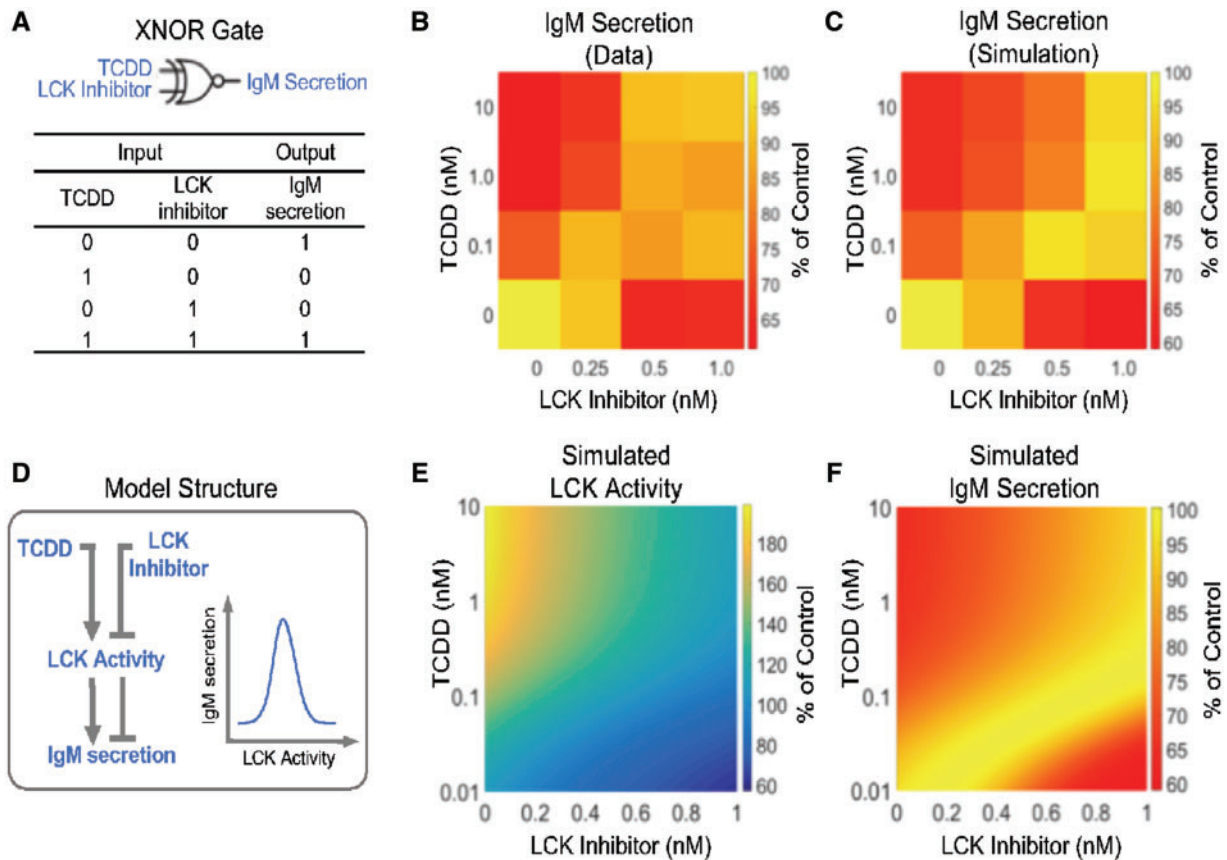


Figure 5. Modeling the XNOR gate effect of TCDD and LCK inhibitor on IgM secretion. (A) The combined effects of TCDD and LCK inhibitor follow an XNOR logic gate phenomenon. (B) Heat map of data showing % suppression of IgM secretion by combinations of TCDD and LCK inhibitor concentrations. (C) Heat map of simulated % inhibition of IgM secretion using the model in (D). (D) The model structure used to emulate an XNOR gate; see text for model details. LCK activity has a biphasic effect on IgM secretion: below an optimal level, as LCK activity increases IgM secretion increases; above the optimal level, as LCK activity increases IgM secretion decreases. (E) Simulated LCK activity under different combinations of TCDD and LCK inhibitor concentrations. (F) Simulated IgM secretion under different combinations of TCDD and LCK inhibitor concentrations.

(Figure 6C). The activation of AHR decreased the percentage of inhibitory pLCK (Tyr505), thereby increasing the ratio of active LCK in B cells (Figs. 6A and 6B). In addition, AHR activation increased active LCK was supported by the increase in the overall level of phosphorylated pZAP70 at Tyr319 and Tyr292 (Figure 7). The percentage of pLCK positive cells did not change with the addition of high affinity LCK inhibitor (Figs. 7A and 7B); however, the addition of LCK inhibitor attenuated the overall level of downstream phosphorylation of pZAP70 (Figs. 7C and 7D). Overall, the effects of TCDD and LCK inhibitor on the activity of LCK, as monitored by ZAP70 phosphorylation, are consistent with that predicted by the XNOR gate model (Figure 5E).

Total Levels of LCK Were Augmented in Responders and Unaffected in Nonresponders Following Treatment With TCDD

Approximately 1 in 7 human donors are “nonresponders” to TCDD treatment as defined by the absence of TCDD-mediated suppression of IgM secretion by B cells from these human donors (Dornbos et al., 2016; Lu et al., 2011). Specifically, responders were classified by a greater than 20% suppression of IgM in the presence of 10 nM TCDD treatment compared with VH control as measured by ELISA and ELISPOT. The explanation for why an individual is nonresponsive to TCDD treatment is still largely unknown. Interestingly, comparing the total LCK expression level between responsive and nonresponsive human donors, with TCDD treatment (10 nM), the level of total LCK

significantly increased in responders (Figs. 8A, 8C, and 8E) while not affected in nonresponders (Figs. 8B, 8D, and 8F).

DISCUSSION

We have recently demonstrated that AHR activation in human B cells results in the impairment of IgM secretion (Zhou et al., 2018). In the present study, we explored the putative involvement of LCK in immunoglobulin secretion. Specifically, we show that LCK, a poorly described signaling protein in B cells, plays a key role in AHR-mediated impairment of IgM secretion.

A previous transcriptomic analysis showed a significant increase in LCK mRNA in AHR-activated human B cells (Kovalova et al., 2017). This observation served as the basis to further investigate the role of LCK in AHR-mediated impairment of humoral immunity. Here we demonstrate significant increases in LCK mRNA and protein that coincide with AHR activation in B cells. This finding has been confirmed using different B-cell activators. The level of total LCK increased with TCDD-mediated AHR activation using various B-cell stimuli suggesting that AHR ligation is critical to LCK upregulation and does not appear to be dependent on the mode of B-cell activation. In the current study, we have observed little LCK expression in naïve resting human B cells (Figure 1B, day 0); however, the level of LCK increases upon B-cell activation. This observation is particularly interesting because LCK is expressed in T cells, in the

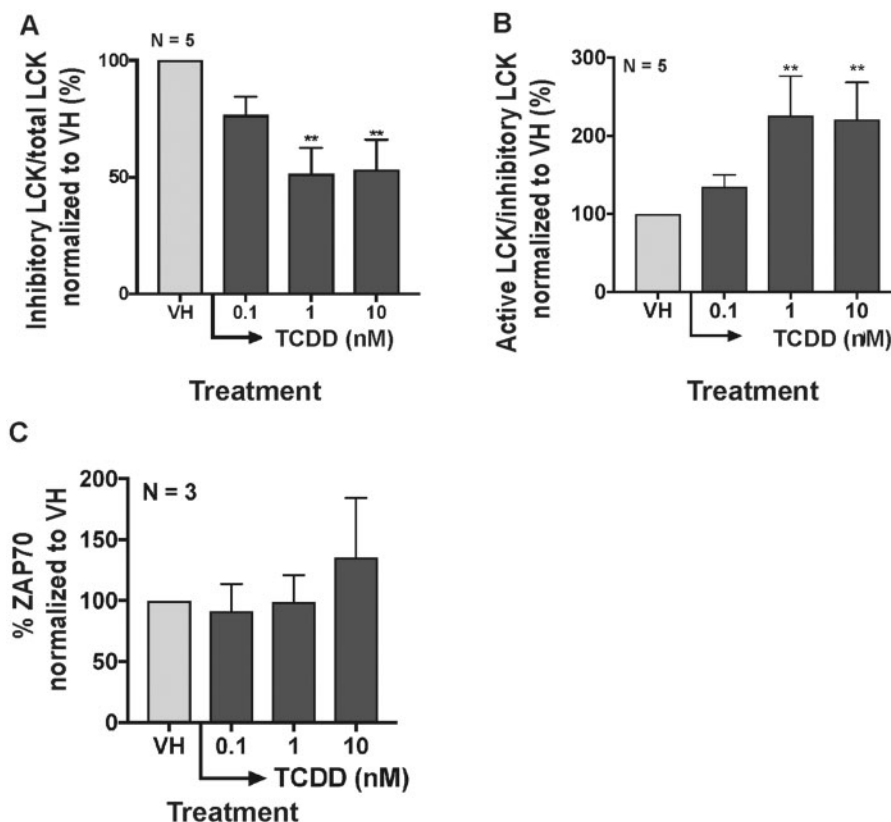


Figure 6. Aryl hydrocarbon receptor activation increased the level of active LCK. B cells were treated with VH (0.02% DMSO) or TCDD (0.1, 1, and 10 nM) and activated by soluble human recombinant CD40 ligand and cytokines (IL-2 and IL-21) for 7 days. (A) Ratio of inhibitory pLCK (Tyr505) versus total LCK and (B) ratio of active pLCK (Tyr505) versus inhibitory pLCK. The ratio was calculated based on the flow cytometry measurement of total LCK and pLCK (Tyr505). (C) Percent total ZAP70⁺ B cells measured by flow cytometry on day 7. Significant differences from VH control are indicated by ** $p < 0.01$ by 1-way ANOVA followed by Fisher's LSD post hoc test. Results are presented as the normalized percentage compared with the VH group. "N" indicates the number of donors used in the study.

absence of activation, and is only modestly increased upon T-cell activation (Koga *et al.*, 1988). Another interesting observation is that the increase in LCK in B cells has little effect on proliferation (Supplementary Figure 1). These observations differ from the known role of LCK in T cells. Specifically, expression of LCK is critical for T-cell proliferation with LCK null mice exhibiting thymic atrophy (van Oers *et al.*, 1996). Likewise, knockout LCK T-cell lines show altered proliferation after activation when compared with the wild-type control expressing LCK T cells (Welte *et al.*, 1999). The late expression of LCK postactivation in human B cells suggests a different role for the protein tyrosine kinase than in T cells. In addition, the modest increase of LCK when TCDD was added to cultures 24 h post B-cell activation suggests that LCK may not be regulated directly by the AHR at the level of transcription (ie, via DREs binding in LCK regulatory regions) but rather through indirect mechanisms (Figure 3). This conclusion is further supported by the observation that LCK upregulation by TCDD, when added at day 0, is most marked on day 3 and continues to increase over the 7-day culture period. Collectively our results suggest an important role for LCK in IgM secretion by human B cells. Interestingly, we also observed a decrease in LCK by treatment of B cells with an AHR antagonist alone, suggesting that endogenous AHR ligand(s) also regulates the expression level of LCK in human B cells, but again likely through an indirect mechanism. Further investigation of the role of LCK in human B cells is necessary.

LCK and LYN belong to the Src kinase family LYN has been well studied in B cells, as it closely associates with the BCR

(Wang *et al.*, 2007). LYN has been shown to interact with SYK in B cells. ZAP70 is found to have similar functions as SYK in T cells. It is clear that there is a redundancy between the LYN-SYK pathway and the LCK-ZAP70 pathway (Oykhman *et al.*, 2013); however, there are few studies describing a role for LCK-ZAP70 in B cells. Based on the transcriptomic study, the significant increase of LCK appears to occur independently of LYN or any Src kinase proteins (LYN, SRC, BLK, and HCK) but is closely linked to AHR activation in humans (Kovalova *et al.*, 2016). In addition, previous studies have shown no changes in the expression level of PAX-5 and BLIMP-1 in TCDD-treated human B cells activated with CD40L plus cytokines, suggesting that activation of the AHR does not alter B-cell differentiation but rather the secretion of immunoglobulin by human B cells (Lu *et al.*, 2011; Zhou *et al.*, 2018). Alternatively, TCDD is exerting effects on a subpopulation of B cells and we lack the sensitivity to detect changes in PAX-5, BLIMP-1, or intracellular IgM in those cells when they are present in the larger pool of CD19⁺ B cells.

The addition of LCK inhibitors restored the AHR-mediated decrease in IgM secretion, indicating that one role for LCK in B cells is either immunoglobulin intracellular trafficking and/or secretion or establishing the necessary intracellular machinery for these processes to take place. Interestingly, treatment with LCK inhibitors alone (Figs. 4G and 4H) impaired the level of IgM secretion, indicating that there is an optimal level of LCK activity required for immunoglobulin secretion. Employing a matrix system, the XNOR model was developed (Figure 5) and verified our results. Based on experimental and

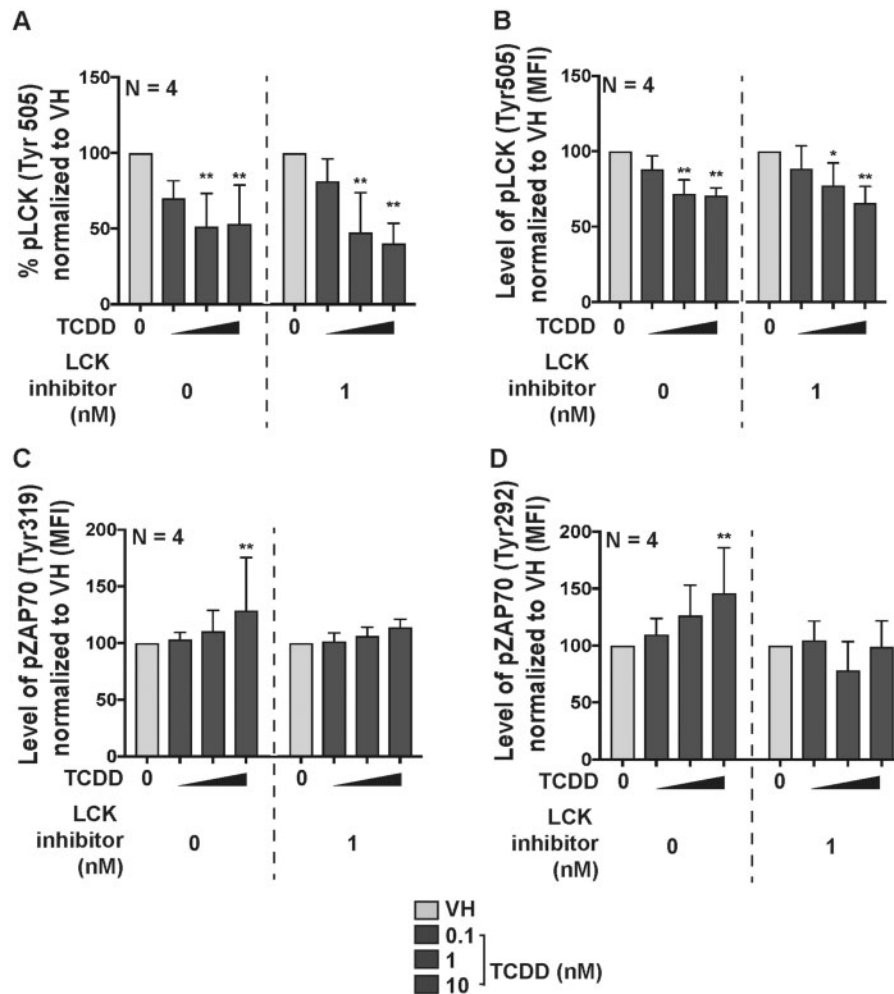


Figure 7. The LCK inhibitor (CAS) attenuated downstream phosphorylation in pZAP70. B cells were treated with VH (0.02% DMSO) or TCDD (10 nM) and activated by soluble human recombinant CD40 ligand and cytokines (IL-2 and IL-21) for 7 days. All samples were measured by flow cytometry. (A) Percent pLCK-Tyr505 positive; (B) levels of pLCK-Tyr505⁺ B cells with or without the addition of LCK inhibitor (CAS 213743-31-8). Significant differences from VH control are indicated by * $p < 0.05$ by 1-way ANOVA followed by Fisher's LSD post hoc test. Results are presented as the normalized percentage compared to the VH group. "N" indicates the number of donors used in the study.

computational observations, the activity of LCK and IgM secretion exhibit a nonmonotonic response (Figure 5D), indicating that, in fact, an optimal level of LCK activity is required for immunoglobulin secretion. To our knowledge this is the first report demonstrating the involvement of LCK in immunoglobulin secretion.

The activity of LCK is governed by phosphorylation of critical tyrosine residues (Hui and Vale, 2014). Because we observed an increase in total LCK levels with AHR activation, it is also important to identify the LCK phosphorylation profile. Antibodies targeting specific phosphorylation sites have provided a better understanding of LCK phosphorylation with TCDD treatment. In the present study, we investigated the phosphorylation of tyrosine 505 (Tyr505), the dominant inhibitory site for LCK (Hui and Vale, 2014). Our studies show that AHR activation decreased the level of phospho-Tyr505 LCK, which is consistent with an overall increase of active LCK (Figure 6B). The downstream increase of ZAP70 phosphorylation on Tyr319 and Tyr292 further verifies the increase of LCK activity (Figure 7). In addition, the change in LCK phosphorylation indicates that AHR activation plays a critical role in modulating the phosphorylation events

in human B cells. The pathways presented in the current study offer a limited snapshot. A more global analysis using phosphoproteomics will be required to provide additional insights on the influence of AHR activation in mediating changes in phosphorylation of critical target proteins in human B cells transitioning from a resting status to antibody secretors.

It has been well documented that B cells from approximately 1 out of the 7 human donors are refractory to suppression of IgM secretion by TCDD treatment (Dornbos et al., 2016; Lu et al., 2011). In the present study, we compared responders and non-responders and observed significant upregulation of LCK in only responsive human donors (Figure 8) suggesting a role of LCK in the impairment of immunoglobulin secretion. Taken together, it is tempting to speculate that LCK could be used as a biomarker to assess sensitivity of a given individual to IgM suppression by TCDD and dioxin-like environmental contaminants.

Recently, it has been reported that human peripheral CD5⁺ B cells characteristically express high levels of LCK as evidenced in CLL patients (Till et al., 2017). CD5⁺ B cells are characterized as innate B cells in both mice and humans. These cells although well defined in the mouse are poorly characterized in the

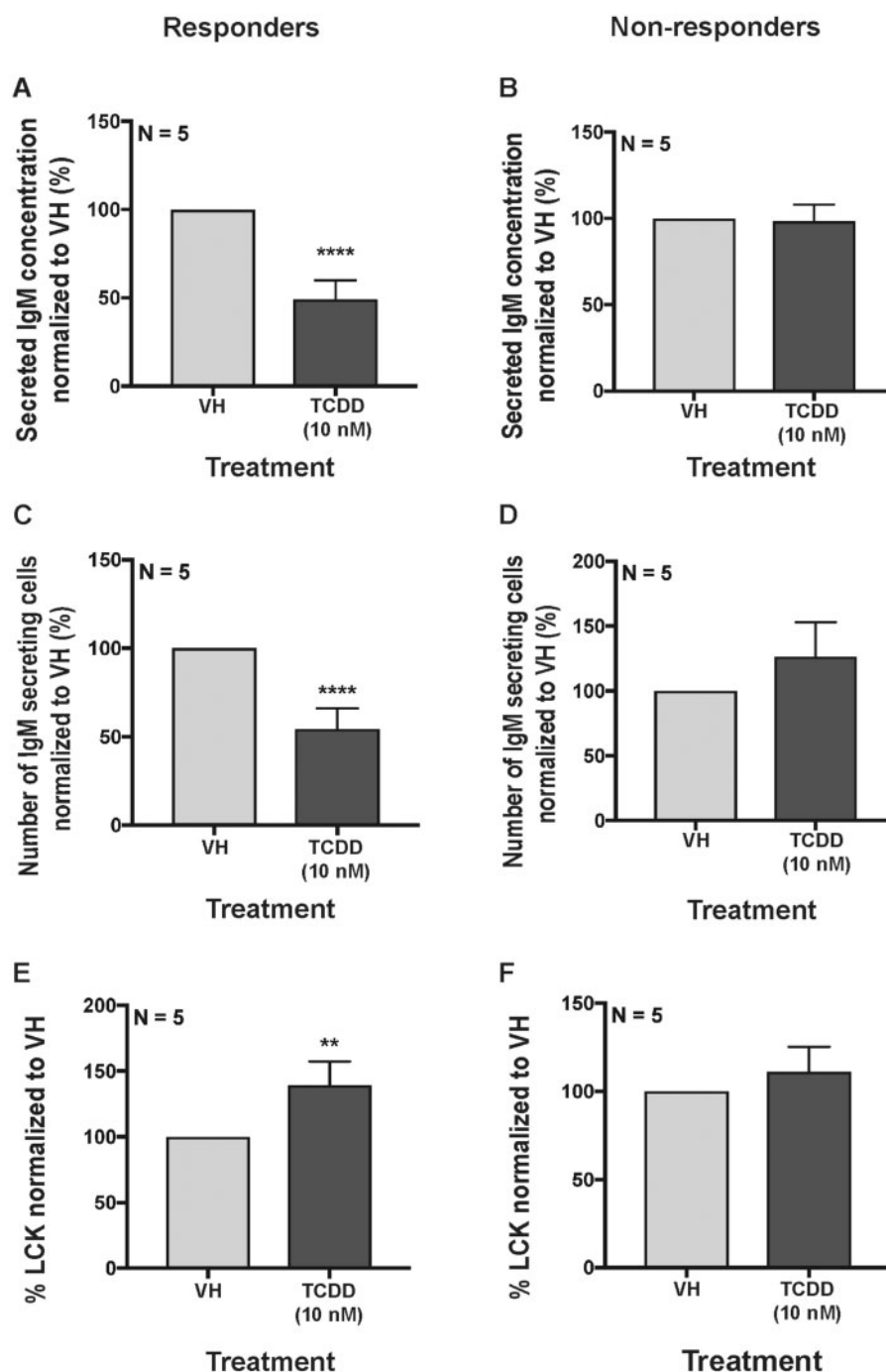


Figure 8. Comparison of total LCK expression levels in responsive and nonresponsive donors. B cells were treated with VH (0.02% DMSO) or TCDD (10 nM) and activated by coculture with CD40 ligand expressing L cells plus cytokines (IL-2, IL-6, and IL-10) for 7 days. The IgM concentration in culture supernatants in (A) responders and (B) nonresponders. Number of IgM secreting B cells in (C) responders and (D) nonresponders. Percent LCK positive human B cells in (E) responders and (F) nonresponders. Significant differences from VH control are indicated by ** $p < 0.01$ and **** $p < 0.0001$ by Student's t-test. Results are presented as the normalized percentage compared with the VH control group. "N" indicates the number of donors used in the study.

human. The high expression of LCK in CD5⁺ human B cells leads us to believe that different B cells subpopulations might have different sensitivity to TCDD treatment. It is tempting to speculate that the expression of total LCK in the CD5⁺ cells in an individual may play a role in the susceptibility and sensitivity to TCDD exposure in the impairment of humoral immunity. Further investigation into the role of LCK in CD5⁺ human B cells could provide important insights concerning sensitive subpopulation to IgM suppression by TCDD.

SUPPLEMENTARY DATA

Supplementary data are available at *Toxicological Sciences* online.

ACKNOWLEDGMENTS

The authors would like to thank Mrs. Kimberly Hambleton for assisting with the submission of this manuscript.

FUNDING

This work was funded by P42 ES004911.

CONFLICT OF INTEREST

The authors report no conflict of interest.

REFERENCES

- Abbott, B. D., Held, G. A., Wood, C. R., Buckalew, A. R., Brown, J. G., and Schmid, J. (1999). AhR, ARNT, and CYP1A1 mRNA quantitation in cultured human embryonic palates exposed to TCDD and comparison with mouse palate in vivo and in culture. *Toxicol. Sci.* **47**, 62–75.
- Barouki, R., Coumoul, X., and Fernandez-Salguero, P. (2007). The aryl hydrocarbon receptor, more than a xenobiotic-interacting protein. *FEBS Lett.* **581**, 3608–3615.
- Bisson, W. H., Koch, D. C., O'Donnell, E. F., Khalil, S. M., Kerkvliet, N. I., Tanguay, R. L., Abagyan, R., and Kolluri, S. K. (2009). Modeling of the aryl hydrocarbon receptor (AhR) ligand binding domain and its utility in virtual ligand screening to predict new AhR ligands. *J. Med. Chem.* **52**, 5635–5641.
- Bunger, M. K., Moran, S. M., Glover, E., Thomae, T. L., Lahvis, G. P., Lin, B. C., and Bradfield, C. A. (2003). Resistance to 2,3,7,8-tetrachlorodibenzo-p-dioxin toxicity and abnormal liver development in mice carrying a mutation in the nuclear localization sequence of the aryl hydrocarbon receptor. *J. Biol. Chem.* **278**, 17767–17774.
- Bunnell, S. C., Hong, D. I., Kardon, J. R., Yamazaki, T., McGlade, C. J., Barr, V. A., and Samelson, L. E. (2002). T cell receptor ligation induces the formation of dynamically regulated signaling assemblies. *J. Cell Biol.* **158**, 1263–1275.
- Di Bartolo, V., Mege, D., Germain, V., Pelosi, M., Dufour, E., Michel, F., Magistrelli, G., Isacchi, A., and Acuto, O. (1999). Tyrosine 319, a newly identified phosphorylation site of ZAP-70, plays a critical role in T cell antigen receptor signaling. *J. Biol. Chem.* **274**, 6285–6294.
- Dornbos, P., Crawford, R. B., Kaminski, N. E., Hession, S. L., and La Pres, J. J. (2016). The influence of human interindividual variability on the low-dose region of dose-response curve induced by 2,3,7,8-tetrachlorodibenzo-p-dioxin in primary B cells. *Toxicol. Sci.* **153**, 352–360.
- Efremov, D. G., Gobessi, S., and Longo, P. G. (2007). Signaling pathways activated by antigen-receptor engagement in chronic lymphocytic leukemia B-cells. *Autoimmun. Rev.* **7**, 102–108.
- Fernandez-Salguero, P. M., Ward, J. M., Sundberg, J. P., and Gonzalez, F. J. (1997). Lesions of aryl-hydrocarbon receptor-deficient mice. *Vet. Pathol.* **34**, 605–614.
- Gonzalez, F. J., and Fernandez-Salguero, P. (1998). The aryl hydrocarbon receptor: studies using the AHR-null mice. *Drug Metab. Dispos.* **26**, 1194–1198.
- Griffin, D. O., Holodick, N. E., and Rothstein, T. L. (2011). Human B1 cells in umbilical cord and adult peripheral blood express the novel phenotype CD20⁺ CD27⁺ CD43⁺ CD70. *J. Exp. Med.* **208**, 67–80.
- Harper, P. A., Prokipcak, R. D., Bush, L. E., Golas, C. L., and Okey, A. B. (1991). Detection and characterization of the Ah receptor for 2,3,7,8-tetrachlorodibenzo-p-dioxin in the human colon adenocarcinoma cell line LS180. *Arch. Biochem. Biophys.* **290**, 27–36.
- Heid, S. E., Pollenz, R. S., and Swanson, H. I. (2000). Role of heat shock protein 90 dissociation in mediating agonist-induced activation of the aryl hydrocarbon receptor. *Mol. Pharmacol.* **57**, 82–92.
- Holsapple, M. P., Dooley, R. K., McNERney, P. J., and McCay, J. A. (1986). Direct suppression of antibody responses by chlorinated dibenzodioxins in cultured spleen cells from (C57BL/6 x C3H)F1 and DBA/2 mice. *Immunopharmacology* **12**, 175–186.
- Hui, E., and Vale, R. D. (2014). In vitro membrane reconstitution of the T-cell receptor proximal signaling network. *Nat. Struct. Mol. Biol.* **21**, 133–142.
- Kerkvliet, N. I. (2002). Recent advances in understanding the mechanisms of TCDD immunotoxicity. *Int. Immunopharmacol.* **2**, 277–291.
- Koga, Y., Kimura, N., Minowada, J., and Mak, T. W. (1988). Expression of the human T-cell-specific tyrosine kinase YT16 (lck) message in leukemic T-cell lines. *Cancer Res.* **48**, 856–859.
- Kovalova, N., Manzan, M., Crawford, R., and Kaminski, N. (2016). Role of aryl hydrocarbon receptor polymorphisms on TCDD-mediated CYP1B1 induction and IgM suppression by human B cells. *Toxicol. Appl. Pharmacol.* **309**, 15–23.
- Kovalova, N., Nault, R., Crawford, R., Zacharewski, T. R., and Kaminski, N. E. (2017). Comparative analysis of TCDD-induced AhR-mediated gene expression in human, mouse and rat primary B cells. *Toxicol. Appl. Pharmacol.* **316**, 95–106.
- Li, J., Bhattacharya, S., Zhou, J., Phadnis-Moghe, A. S., Crawford, R. B., and Kaminski, N. E. (2017). Aryl hydrocarbon receptor activation suppresses EBF1 and PAX5 and impairs human B lymphopoiesis. *J. Immunol.* **199**, 3504–3515.
- Li, J., Phadnis-Moghe, A. S., Crawford, R. B., and Kaminski, N. E. (2017). Aryl hydrocarbon receptor activation by 2,3,7,8-tetrachlorodibenzo-p-dioxin impairs human B lymphopoiesis. *Toxicology* **378**, 17–24.
- Lu, H., Crawford, R. B., Kaplan, B. L., and Kaminski, N. E. (2011). 2, 3, 7, 8-Tetrachlorodibenzo-p-dioxin-mediated disruption of the CD40 ligand-induced activation of primary human B cells. *Toxicol. Appl. Pharmacol.* **255**, 251–260.
- Majolini, M. B., D'Elisio, M. M., Galienu, P., Boncristiano, M., Lauria, F., Del Prete, G., Telford, J. L., and Baldari, C. T. (1998). Expression of the T-cell-specific tyrosine kinase Lck in normal B-1 cells and in chronic lymphocytic leukemia B cells. *Blood* **91**, 3390–3396.
- Mimura, J., Ema, M., Sogawa, K., and Fujii-Kuriyama, Y. (1999). Identification of a novel mechanism of regulation of Ah (dioxin) receptor function. *Genes Dev.* **13**, 20–25.
- Nguyen, L. P., and Bradfield, C. A. (2008). The search for endogenous activators of the aryl hydrocarbon receptor. *Chem. Res. Toxicol.* **21**, 102–116.
- Nguyen, N., Hanieh, H., Nakahama, T., and Kishimoto, T. (2013). The roles of aryl hydrocarbon receptor in immune responses. *Int. Immunol.* **25**, 335–343.
- North, C. M., Crawford, R. B., Lu, H., and Kaminski, N. E. (2010). 2, 3, 7, 8-tetrachlorodibenzo-p-dioxin-mediated suppression of toll-like receptor stimulated B-lymphocyte activation and initiation of plasmacytic differentiation. *Toxicol. Sci.* **116**, 99–112.
- Oykhman, P., Timm-McCann, M., Xiang, R. F., Islam, A., Li, S. S., Stack, D., Huston, S. M., Ma, L. L., and Mody, C. H. (2013). Requirement and redundancy of the Src family kinases Fyn and Lyn in perforin-dependent killing of *Cryptococcus neoformans* by NK cells. *Infect. Immunity* **81**, 3912–3922.
- Perdew, G. H. (1988). Association of the Ah receptor with the 90-kDa heat shock protein. *J. Biol. Chem.* **263**, 13802–13805.

- Phadnis-Moghe, A. S., Chen, W., Li, J., Crawford, R. B., Bach, A., D'Ingillo, S., Kovalova, N., Suarez-Martinez, J. E., Kaplan, B. L. F., Harrill, J. A., et al. (2016). Immunological characterization of the aryl hydrocarbon receptor (AHR) knockout rat in the presence and absence of 2,3,7,8-tetrachlorodibenzo-p-dioxin (TCDD). *Toxicology* **368–369**, 172–182.
- Poland, A., and Knutson, J. C. (1982). 2, 3, 7, 8-tetrachlorodibenzo-p-dioxin and related halogenated aromatic hydrocarbons: Examination of the mechanism of toxicity. *Annu. Rev. Pharmacol. Toxicol.* **22**, 517–554.
- Roskoski, R., Jr. (2005). Src kinase regulation by phosphorylation and dephosphorylation. *Biochem. Biophys. Res. Commun.* **331**, 1–14.
- Schmidt, J. V., Su, G. H., Reddy, J. K., Simon, M. C., and Bradfield, C. A. (1996). Characterization of a murine Ahr null allele: involvement of the Ah receptor in hepatic growth and development. *Proc. Natl. Acad. Sci. USA.* **93**, 6731–6736.
- Schneider, D., Manzan, M. A., Crawford, R. B., Chen, W., and Kaminski, N. E. (2008). 2,3,7,8-Tetrachlorodibenzo-p-dioxin-mediated impairment of B cell differentiation involves dysregulation of paired box 5 (Pax5) isoform, Pax5a. *J. Pharmacol. Exp. Ther.* **326**, 463–474.
- Shi, X., Bi, Y., Yang, W., Guo, X., Jiang, Y., Wan, C., Li, L., Bai, Y., Guo, J., Wang, Y., et al. (2013). Ca²⁺ regulates T-cell receptor activation by modulating the charge property of lipids. *Nature* **493**, 111–115.
- Smith, B. W., Rozelle, S. S., Leung, A., Ubellacker, J., Parks, A., Nah, S. K., French, D., Gadue, P., Monti, S., Chui, D. H., et al. (2013). The aryl hydrocarbon receptor directs hematopoietic progenitor cell expansion and differentiation. *Blood* **122**, 376–385.
- Sorg, O. (2014). AhR signalling and dioxin toxicity. *Toxicol. Lett.* **230**, 225–233.
- Sulentic, C. E., and Kaminski, N. E. (2011). The long winding road toward understanding the molecular mechanisms for B-cell suppression by 2,3,7,8-tetrachlorodibenzo-p-dioxin. *Toxicol. Sci.* **120**, S171–S191.
- Talab, F., Allen, J. C., Thompson, V., Lin, K., and Slupsky, J. R. (2013). LCK is an important mediator of B-cell receptor signaling in chronic lymphocytic leukemia cells. *Mol. Cancer Res.* **11**, 541–554.
- Thurmond, T. S., Staples, J. E., Silverstone, A. E., and Gasiewicz, T. A. (2000). The aryl hydrocarbon receptor has a role in the in vivo maturation of murine bone marrow B lymphocytes and their response to 2,3,7,8-tetrachlorodibenzo-p-dioxin. *Toxicol. Appl. Pharmacol.* **165**, 227–236.
- Till, K. J., Allen, J. C., Talab, F., Lin, K., Allsup, D., Cawkwell, L., Bentley, A., Ringshausen, I., Duckworth, A. D., Pettitt, A. R., et al. (2017). Lck is a relevant target in chronic lymphocytic leukaemia cells whose expression variance is unrelated to disease outcome. *Sci. Rep.* **7**, 16784.
- Tucker, A. N., Vore, S. J., and Luster, M. I. (1986). Suppression of B cell differentiation by 2,3,7,8-tetrachlorodibenzo-p-dioxin. *Mol. Pharmacol.* **29**, 372–377.
- van Oers, N. S., Lowin-Kropf, B., Finlay, D., Connolly, K., and Weiss, A. (1996). alpha beta T cell development is abolished in mice lacking both Lck and Fyn protein tyrosine kinases. *Immunity* **5**, 429–436.
- Veldhoen, M., Hirota, K., Christensen, J., O'Garra, A., and Stockinger, B. (2009). Natural agonists for aryl hydrocarbon receptor in culture medium are essential for optimal differentiation of Th17 T cells. *J. Exp. Med.* **206**, 43–49.
- Veldhoen, M., Hirota, K., Westendorf, A. M., Buer, J., Dumoutier, L., Renaud, J. C., and Stockinger, B. (2008). The aryl hydrocarbon receptor links TH17-cell-mediated autoimmunity to environmental toxins. *Nature* **453**, 106–109.
- Vorderstrasse, B. A., Stepan, L. B., Silverstone, A. E., and Kerkvliet, N. I. (2001). Aryl hydrocarbon receptor-deficient mice generate normal immune responses to model antigens and are resistant to TCDD-induced immune suppression. *Toxicol. Appl. Pharmacol.* **171**, 157–164.
- Wang, H., Kadlecsek, T. A., Au-Yeung, B. B., Goodfellow, H. E., Hsu, L. Y., Freedman, T. S., and Weiss, A. (2010). ZAP-70: an essential kinase in T-cell signaling. *Cold Spring Harb. Perspect. Biol.* **2**, a002279.
- Wang, L., Kurosaki, T., and Corey, S. J. (2007). Engagement of the B-cell antigen receptor activates STAT through Lyn in a Jak-independent pathway. *Oncogene* **26**, 2851–2859.
- Welte, T., Leitenberg, D., Dittel, B. N., al-Ramadi, B. K., Xie, B., Chin, Y. E., Janeway, C. A., Jr., Bothwell, A. L., Bottomly, K., and Fu, X. Y. (1999). STAT5 interaction with the T cell receptor complex and stimulation of T cell proliferation. *Science* **283**, 222–225.
- Whitlock, J. P., Jr. (1990). Genetic and molecular aspects of 2, 3, 7, 8-tetrachlorodibenzo-p-dioxin action. *Annu. Rev. Pharmacol. Toxicol.* **30**, 251–277.
- Zhou, J., Henriquez, J., Crawford, R., and Kaminski, N. (2018). Suppression of the IgM response by Aryl hydrocarbon receptor activation in human primary B cells involves impairment of immunoglobulin secretory processes. *Toxicol. Sci.* **163**(1), 319–329.